Proton-proton elastic scattering excitation functions at intermediate energies*

published in *Phys. Rev. Lett.* **78**, 1652 (1997)

D. Albers[2], J. Bisplinghoff[1], R. Bollmann[2], K. Büßer[2], P. Cloth[3], R. Daniel[1], O. Diehl[1], F. Dohrmann[2], H.P. Engelhardt[1], J. Ernst[1], P.D. Eversheim[1], M. Gasthuber[2], R. Gebel[3], J. Greiff[2], A. Groß[2], R. Groß-Hardt[1], S. Heider[1], A. Heine [1], F. Hinterberger[1], M. Igelbrink[2], R. Jahn[1], M. Jeske[1], U. Lahr[1], R. Langkau[2], J. Lindlein[2], R. Maier[3], R. Maschuw[1], T. Mayer-Kuckuk[1], F. Mosel[1], M. Müller[2], M. Münstermann[2], D. Prasuhn[3], H. Rohdjeß[1], D. Rosendaal[1], U. Roß[1], P. von Rossen[3], H. Scheid[1], N. Schirm[2], M. Schulz-Rojahn[1], F. Schwandt[1], V. Schwarz[1], W. Scobel[2], G. Sterzenbach[3], H.J. Trelle[1], A. Wellinghausen[2], W. Wiedmann[1], K. Woller[2], R. Ziegler[1]

(1) Inst. f. Strahlen- und Kernphysik, Univ. Bonn
(2) I. Inst. f. Experimentalphysik, Univ. Hamburg
(3) Inst. f. Kernphysik, KFA Jülich
(EDDA-collaboration)

(Received 8 November 1996)

Excitation functions of proton–proton elastic scattering cross sections have been measured in narrow steps for projectile momenta p_p (energies T_p) from 1100 MeV/c to 3300 MeV/c (500 MeV to 2500 MeV) in the angular range 35° $\leq \Theta_{c.m.} \leq$ 90° with a detector providing $\Delta\Theta_{c.m.} \approx$ 1.4° resolution. Measurements have been performed continuously during projectile acceleration in the Cooler Synchrotron COSY with an internal CH_2 fiber target, taking particular care to monitor luminosity as a function of T_p. The advantages of this experimental technique are demonstrated, and the excitation functions obtained are compared to existing cross section data. No evidence for narrow structures was found.

PACS numbers: 25.40.Cm, 13.75.Cs, 21.30.Cb, 25.40.Ve

Elastic nucleon–nucleon scattering is a process fundamental to understanding nuclear forces. Its knowledge also forms the basis of a broad range of applications in nuclear and heavy ion physics, e.g. as ingredients to models of reaction dynamics, excited nuclear matter and transport phenomena. Consequently, many experimental and theoretical studies (see [1–5] and refences therein) have been devoted to the subject. The data base has doubled over the last decade [6,7], and global phase shifts now extend to 1600 MeV (1300 MeV) in kinetic beam energy for pp (np) scattering [7].

Closer inspection shows, however, that the vast majority of data is below 1460 MeV/c (800 MeV) of momentum (kinetic energy). They are, with a few exceptions [8–10], angular distributions for discrete energies whose uncertainties of relative normalization [11] will propagate through phase shifts into the resulting nucleon–nucleon potentials [12]. Above that, the data base grows increasingly sparse, even for spin averaged cross sections.

The advent of proton cooler synchrotrons with internal target stations and beams of up to 3300 MeV/c in momentum p_p [13,14] offers the possibility of drastic improvements on this situation. The high luminosities obtained with the recirculating synchrotron beam provide for pp measurements with unprecedented efficiency, which translates into a high degree of precision and statistical accuracy. This advantage is exploited by the EDDA experiment [15] to be reported here, in several ways:

- First, pp data can be taken at small (some MeV/c) increments of p_p, giving nearly continuous excitation functions. Apart from substantially advancing the data base for, e.g., consistent phase shift analyses, this offers great sensitivity to deviations from a smooth energy dependence [9,10,16], whatever such deviations may indicate.
- Second, the recirculating internal synchrotron beam requires (and allows for) thin targets [17]. This has the additional advantage that electrons from p–e scattering emerge nearly undisturbed and can thus be used for luminosity monitoring and a reliable normalization.
- Third, measurements can be made during synchrotron acceleration in a multipass technique [8], virtually eliminating all systematic errors resulting from long term drifts such as, e.g., target degradation.
- Finally, the cleanest of polarized proton targets, a polarized atomic beam, can be used due to the high resulting beam current. In conjunction with a polarized synchrotron beam, a considerable number of spin observables can then be measured.

Such benefits come at a price, however. Beam, target and detector properties have to be matched closely, and extensive beam monitoring is required. It is the purpose of this Letter to demonstrate the feasibility of the method and its potential, with the example of the first results obtained by EDDA, namely differential cross sections measured with an internal 4 μm·5 μm CH_2 fiber target.

The EDDA experiment uses the cooler synchrotron COSY [13], taking advantage of the remarkable quality and stability which the internal COSY beam offers.

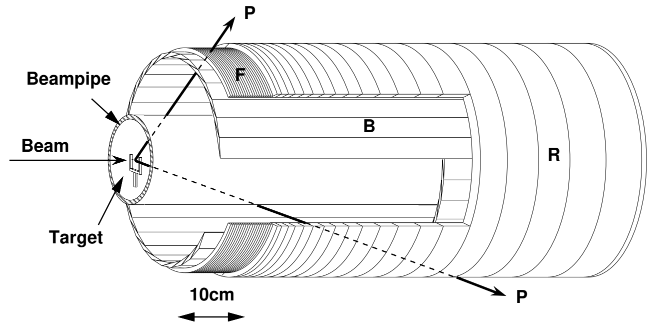

FIG. 1. The EDDA detector (not to scale): **Target** fiber (CH_2), later a polarized atomic hydrogen beam; beampipe (2mm Al in the solid angle covered); **B** scintillator bars; **R** scintillator semi-rings; **F** semi-rings from scintillating fibers.

Data collection proceeds **during synchrotron acceleration** from 1100 to 3300 MeV/c of momentum, such that a complete excitation function is measured during each acceleration cycle. Statistical accuracy is obtained by averaging over many cycles. The sizes of energy and angle binning may be chosen offline in accordance with the progress and resolution of the experiment.

The detector concept is shown in Fig. 1 in a schematic fashion. It is based on a fast triggering of coplanar two–prong events of charged particles that fulfill the kinematic relation between the laboratory angles Θ_{lab}^{p1} and Θ_{lab}^{p2} for elastic proton–proton scattering, viz.

$$\tan\Theta_{lab}^{p1} \cdot \tan\Theta_{lab}^{p2} = 2m_pc^2/(T_p + 2m_pc^2) \qquad (1)$$

where m_p is the proton rest mass. The detector consists of a cylindrical double layer that surrounds the thin walled beampipe downstream from the horizontally oriented fiber target. The angular range covered extends from $\Theta_{lab} = 10°$ to $72°$ subtending 85% of the solid angle. The outer layer consists of 32 scintillator bars (B in Fig. 1) with readout at both ends which are running parallel to the beam axis; they are surrounded by scintillator semi–rings (R). The scintillators are in both layers partially overlapping; their cross sections have been designed such that each particle from the vertex traversing the outer layer deposits energy in two adjacent bars and two semi–rings. Analysis of the fractional light output is then used [18] to determine the point of incidence by a factor of 5 more accurately than it is possible on the basis of detector granularity alone, yielding resolutions 1.0° (1.9°) (FWHM) in $\Theta_{c.m.}(\Phi_{c.m.})$. For angles $\Theta_{lab} > 52°$, the resolution in $\Theta_{c.m.}$ is obtained with semirings of a scintillating fiber (F) structure [19].

Fig. 2 illustrates the identification of elastic proton–proton scattering in the peak of the kinematic coincidence. Quasielastic background due to the carbon content of the CH_2 fiber target results in a structureless distribution that has been measured separately with a pure carbon fiber target. For each event from the CH_2 or the C target with a minimum of two prongs, the angular de-

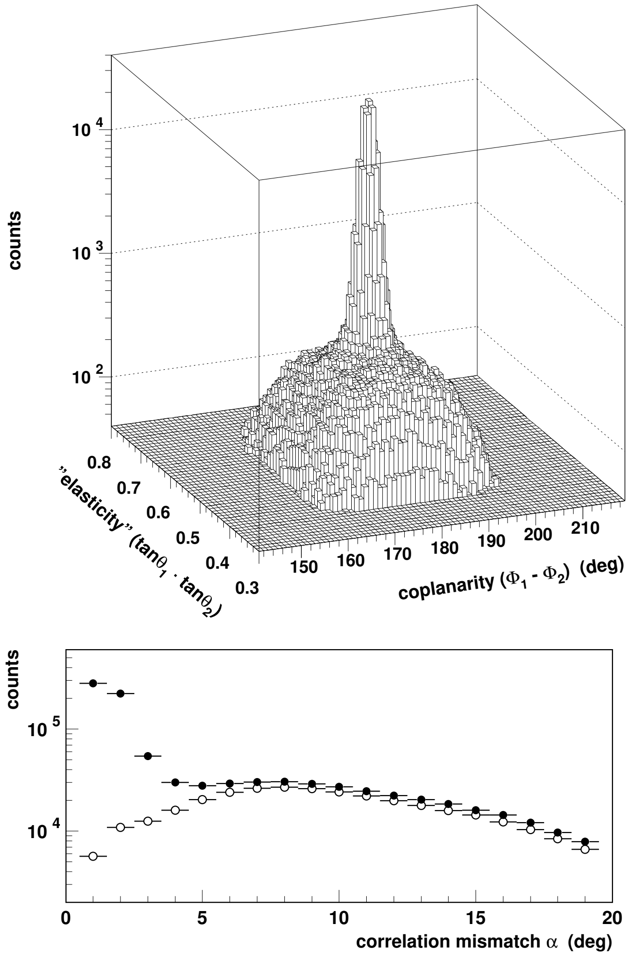

FIG. 2. Top: Kinematic distribution of angle integrated EDDA events as obtained with a CH_2 fiber target at p_p = 2250 MeV/c. Please note the logarithmic scale.
Bottom: Distribution of correlation mismatch angle α for measurements with a CH_2 (closed symbols) and a carbon (open) fiber target. Data are not yet normalized to the same luminosity.

viation α from the expected 180° correlation in the c.m. is deduced under the assumption of elastic pp scattering kinematics. The distribution of this correlation mismatch α in Fig. 2 shows that elastic pp events clearly stand out for $\alpha \leq 6°$. Monte Carlo simulations show that the α distribution of inelastic pp-reactions (e.g. pp$\rightarrow$ pnπ^+, $\rightarrow$pp$\pi^+\pi^-$, $\rightarrow$ppπ°) is similar to that for p+C but at least an order of magnitude less intense. Therefore the nonelastic background below the peak is subtracted by normalizing the distribution of the C events to that of the CH_2 events in the interval $8° \leq \alpha \leq 15°$; extension to higher angles yields the same normalization within the statistical uncertainties. This background correction amounts for $\alpha \leq 8°$ to 5% – 45%, depending on p_p and scattering angle; the resulting statistical uncertainty is largest at high p_p and $\Theta_{c.m.}^{p1} = \Theta_{c.m.}^{p2} = 90°$ where the pp scattering cross section is smallest. Monte Carlo calculations of the detector efficiency yield that with a cut $\alpha \leq 8°$ only $\approx 1\%$ of all true elastic pp events are lost. The Monte Carlo based correction for reaction losses of scattered protons in the detector material is $\leq 3\%$.

Measurements were performed with about 10^7 protons circulating in COSY with a gaussian beam width of $\Delta_{hor} \approx 3$ mm and $\Delta_{vert} \approx 5$ mm (FWHM) at the target position. Data collection proceeded during proton acceleration with constant momentum growth $\Delta p_p/\Delta t$ = 1.15 GeV·c/s and an average luminosity of typically $5 \cdot 10^{29}$ cm^{-2}s^{-1}. The instantaneous projectile momentum was derived from the radio frequency and the known circumference of the synchrotron with an uncertainty of less than 0.25 MeV/c (2 MeV/c) for the lowest (highest) momentum under study. Beam position and width were monitored using both COSY diagnostic tools and the data itself with an uncertainty of less than one mm; they were remarkably reproducible and stable during acceleration, with the position shifting no more than about 3 mm. Adiabatic cooling (due to acceleration) and heating of the beam (due to the target) could be made to balance each other [20], so that measurements could be carried out at near constant emittance and luminosity.

Relative normalization with respect to energy dependence was accomplished by concurrent measurements of the total yield of scecondary electrons emanating from the target, and of the δ–electrons from the elastic p–e scattering. The secondary electron monitor (SEM) consists of a fast amperemeter measuring the current of electrons from ground to target fiber, replacing those knocked out by beam particles. To this end a very thin aluminum film (20 μg/cm^2) was evaporated onto the fiber targets to make them electrically conducting. The δ-electrons were detected in four silicon detectors at Θ_{lab} = 40° located behind thin windows in the beam pipe. The two methods are essentially independent, as the first one scales as the energy deposited in the target, the other as the Rosenbluth cross section. They give the same normalization within 2.5% for all energies. The data presented here refer to SEM monitoring.

Absolute normalization is established at p_p=1455 MeV/c with reference to the angular distribution measured by Simon et al. [11] in an external experiment with 1% total uncertainty. Fig. 3 shows the good agreement of our cross sections for the interval $\Theta_{c.m.}$=88°–90° with those of the fixed angle (Θ_{lab}=40.4°) experiment [8] performed inside the accelerator Saturne with multipass technique, too; our data extend beyond the energy region of overlap with a smooth energy dependence, whereas data of single energy runs taken from the SAID compilation [7] scatter considerably.

Some examples of the data obtained are shown in Figs. 3 and 4 in the form of excitation functions and angular distributions and compared to data from the literature. Our present analysis is based on a total of $2 \cdot 10^7$ elastic pp events that are grouped in 28 MeV/c wide bins in

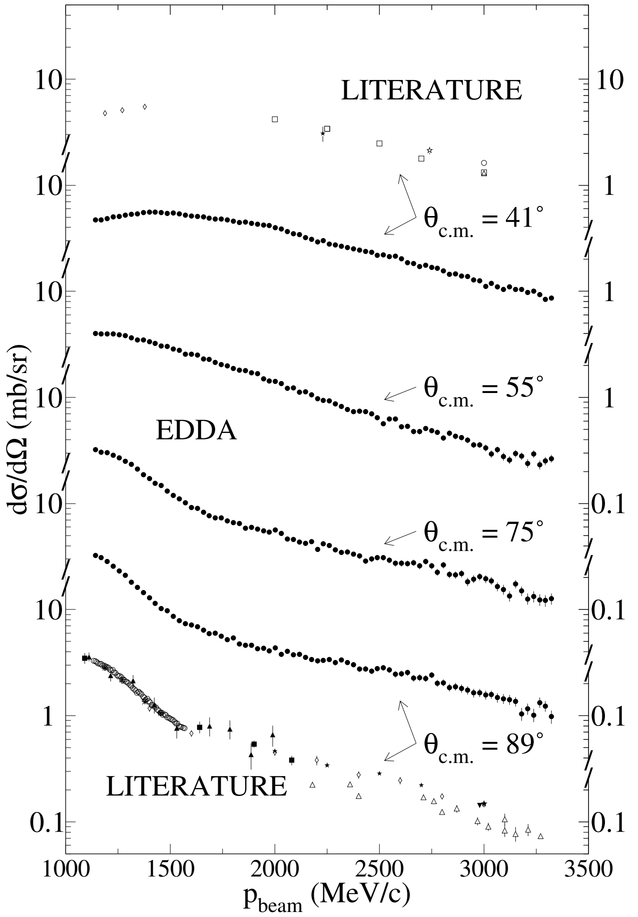

FIG. 3. Excitation functions for elastic pp-scattering: EDDA results for Θ_{cm} = 41°± 1° , 55°± 1°, 75°± 1° and 89°± 1°. For the two extreme angles all data compiled in ref. [7], including the excitation function from [8], are shown in comparison.

beam momentum. As can be seen from the figures, the EDDA data cover the energy and angle domain under study much more extensively and to a much higher degree of accuracy than existing data. In fact, for most of the cross sections measured by EDDA, no data are available in the literature for comparison.

The cross sections measured show a smooth dependence on both angle and energy. No structure has been observed which could be taken as evidence for a resonant excursion. Especially at p = 2900 MeV/c (T_p = 2110 MeV) where a narrow structure in the excitation function of the polarization correlation A_{NN} has been observed [16] we do not see any anomaly in our data. The sensitivity of the elastic scattering observables to an isolated Breit–Wigner resonance has been tested by supplementing the phase shifts from [7] for one of the partial waves $^1S_0$, $^1D_2$ with a corresponding term. From these tests we deduce a typical limit of 0.1 for the elasticity $(2J+1)\Gamma_{\rm el}/\Gamma$. Here, J is the spin and $\Gamma_{\rm el}$ and Γ are the elastic width and total width, respectively, with Γ ranging from $\approx$ 25 MeV – 100 MeV.

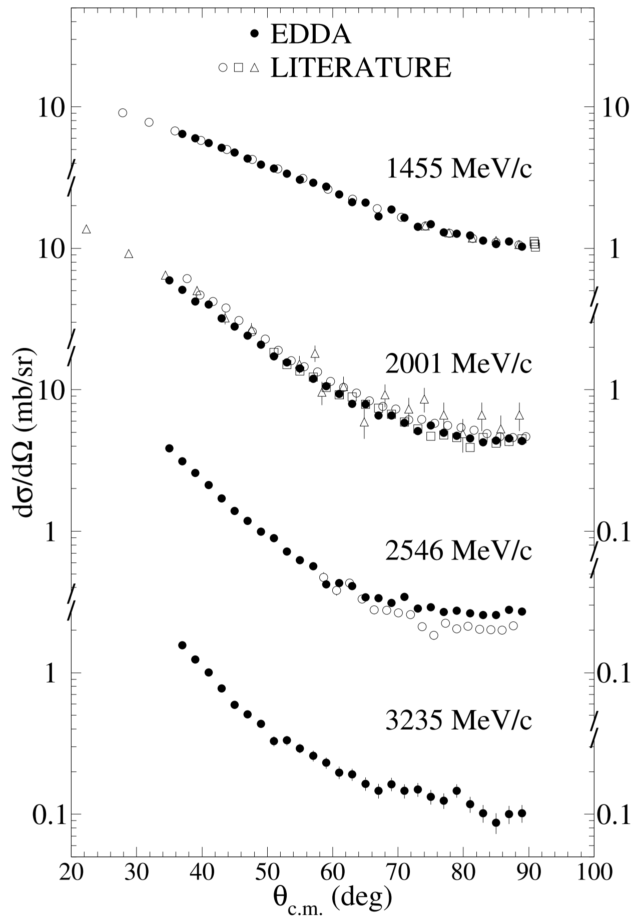

FIG. 4. Angular distributions: Representative results for 28 MeV/c bins from the present work in comparison to all data from the compilation [7].

The smooth momentum dependence of the cross sections found here allows a reliable interpolation between our data. This is important, because spin observables to be determined later in the course of the EDDA experiment can be expressed as bilinear products of scattering amplitudes divided by the scattering cross sections $d\sigma/d\Omega$; therefore the latter enter repeatedly into phase shift analyses.

To summarize, the EDDA experiment provides at present consistent proton–proton elastic scattering cross sections covering 35° to 90° in c.m. scattering angle and 1100 to 3300 MeV/c in projectile momentum in small steps, to a precision of typically 5 % depending on kinematic region and size of binning. Refined data analysis, including recent additional $2{\cdot}10^7$ data, is striving to achieve 2 % relative precision in p_p and $\Theta_{c.m.}$ dependence, and a more stringent limit to the existence of resonant excursions. The method of using the internal synchrotron beam during acceleration works well and can now be exploited to measure spin observables with a polarized atomic beam target. At present preparations for measurements with polarized projectiles and a polarized atomic gas target are under way [21] including the equipment of the detector with an additional inner layer for vertex reconstruction. Data of pp analyzing powers and spin correlation coefficients for $p_p > 1460$ MeV/c are very scarce and partly inconsistent [5,7], and it is obvious that the extension of the EDDA experiment to their measurement will improve this situation considerably and have impact on phase shift analyses [22].

The EDDA collaboration gratefully acknowledges the extraordinary support and collaboration received from the COSY accelerator group.

---

* Work supported by the BMBF, contracts 06BN664I(6) and 06HH561Tp2, and by the Forschungszentrum Jülich, contracts FFE41126803 and FFE41126903.

[1] C. Elster et al., Phys. Rev. **C38**,1828 (1988).
[2] R. Vinh Mau et al., Phys. Rev. Lett. **67**,1392 (1991).
[3] R. Machleidt et al., Phys. Rep. **149**,1 (1987).
[4] Y. Fujiwara et al., Phys. Rev. Lett. **76**,2242 (1996).
[5] C. Lechanoine–Leluc and F. Lehar, Rev. Mod. Phys. **65**,47 (1993).
[6] R.A. Arndt et al., Phys. Rev. **D28**,97 (1983).
[7] R.A. Arndt et al., Phys. Rev. **C50**,2731 (1994); solution SM95.
[8] M. Garçon et al., Nucl. Phys. **A445**,669 (1985).
[9] R. Beurtey et al., Phys. Lett. **B293**,27 (1992).
[10] Y. Kobayashi et al., Nucl. Phys. **A569**,791 (1994).
[11] A.J. Simon et al., Phys. Rev. **C48**,662 (1993); **C53**,30 (1996).
[12] H. Leeb and D. Leidinger, Few Body Syst. Suppl. **6**,117 (1992).
[13] R. Maier et al., Proc. Int. Conf. on Physics with GeV-Particle Beams (Jülich, Germany, 1994)p. 507.
[14] D. Reistad, Phys. Scripta **48**,37 (1993).
[15] J. Bisplinghoff and F. Hinterberger, AIP Conf. Proc. **221**,312 (1991); W. Scobel, Phys. Scripta **48**,92 (1993); H. Rohdjeß, Proc. Int. Conf. on Physics with GeV-Particle Beams (Jülich 1994), p.334.
[16] J. Ball et al., Phys. Lett. **B320**,206 (1994).
[17] C. Ekström, Nucl. Instr. and Meth. **A362**,1 (1996).
[18] J. Bisplinghoff et al., Nucl. Instr. and Meth. **A329**,151 (1993); K. Ackerstaff et al., Nucl. Instr. and Meth. **A335**,113 (1993).
[19] D. Albers et al., Nucl. Instr. and Meth. **A371**,388 (1996).
[20] F. Hinterberger and D. Prasuhn, Nucl. Instr. and Meth. **A321**,453 (1992).
[21] A. Lehrach, in *Proceedings of the Spin Conference, Amsterdam, 1996*, edited by T. Ketel (World Scientific, Singapore, 1997); P.D. Eversheim, in *Polarized Ion Sources and Polarized Gas Targets*, edited by L.W. Anderson and W. Haeberli, AIP Conf. Proc. No. 293 (1993),p.92.
[22] M. Sander and H.V. von Geramb, Few Body Problems in Physics, AIP Conf. Proc. **334**,825 (1995).